Thermal energy storage system for efficient diesel exhaust aftertreatment at low temperatures

Hamedi, Mohammadreza; Doustdar, Omid; Tsolakis, Athanasios; Hartland, Jonathan

DOI:
10.1016/j.apenergy.2018.11.008

THERMAL ENERGY STORAGE SYSTEM FOR EFFICIENT DIESEL EXHAUST AFTERTREATMENT AT LOW TEMPERATURES

M.R. Hamedi[1], O. Doustdar[1], A. Tsolakis[1,*], J. Hartland[2]

Abstract

To reduce cold-start emissions, a thermal energy storage (TES) system can be used in conjunction with the exhaust aftertreatment system. Phase change materials (PCM) can be used in the TES system to absorb the exhaust gas thermal energy, thus liquefying and storing it as latent heat. This allows storage of the exhaust gas thermal energy during the engine's high-load conditions and gradually releases the thermal energy back to the catalyst substrate during the engine-off period.

Based on the results, implementing a TES system into the diesel aftertreatment system has shown great potential in reducing a vehicle's emissions, particularly for hybrid vehicles. This approach can assist the catalyst to activate the emissions' conversion reactions straight after the cold-start. However, its effectiveness largely depends on the duration of the engine-off periods between the driving cycles. In this study, it was found that facilitating the heat transfer between the PCM and the catalyst can significantly improve the emissions' reduction performance by avoiding the catalyst to light-out after the cold-start.

A substantial improvement in the system's thermal behaviour was observed by using PCM additives and metallic catalyst substrates to increase the system's thermal conductivity. Although a TES system increases the aftertreatment cost and complexity, it can result in substantial emissions' reduction over the vehicle's operating life. This can also translate into reduced vehicle fuel consumption and CO_2 emissions, as the emissions-related fuel penalty will be minimized.

Keywords: thermal management, diesel aftertreatment, engine cold-start, phase change material, catalytic converter, emissions

---

[1] Department of Mechanical Engineering, School of Engineering, University of Birmingham, Birmingham B15 2TT, UK

[2] Powertrain Research and Technology, Jaguar Land Rover, Coventry, UK

[*] Corresponding author, E-mail: a.tsolakis@bham.ac.uk Tel: +44 (0) 121 414 4170 Fax: +44 (0) 121 414 7484

1. Introduction

Emissions' control technologies have substantially developed to fulfil the stringent emissions' regulations since the first introduction of a catalytic converter. Different aftertreatment technologies, i.e. DOC (diesel oxidation catalyst), SCR (selective catalytic reduction) and DPF (diesel particulate filter) can reduce diesel engines' emissions by oxidizing CO and HC, reducing NO_x, then filtering and oxidizing PM emissions [1-3]. These aftertreatment systems have been developed over the past decades to reduce the required activation energy for emissions' conversion reactions [4].

However, recent advances in IC engines have limited the thermal energy available for the aftertreatment systems to effectively reduce the diesel engines' emissions. Different engine-based heating strategies are used to provide more thermal energy to the aftertreatment catalysts for an improved emissions' reduction performance, particularly during a cold-start [5-7]. In these strategies, the engine is calibrated to less efficient conditions to increase its exhaust gas temperature for aftertreatment systems; this can also assist in lowering engines' NO_x emissions [8]. However, engine-based catalyst heating strategies generally lead to increased fuel consumption and CO_2 emissions.

Exhaust gas aftertreatment systems are typically ineffective during an engine's cold-start; thus, releasing a high proportion of the vehicle's emissions during this period [9, 10]. This highlights the need for the thermal management of aftertreatment systems for maximum emissions' reduction, particularly during the engine's cold-start and low-load conditions [3].

To reduce the cold-start emissions, a thermal energy storage (TES) system can be used in conjunction with the exhaust aftertreatment system. Phase change materials (PCM) can be used in the TES system to absorb the exhaust gas thermal energy; thus, liquefying and storing it as latent heat [11, 12]. The PCMs offer relatively high energy storage density at a constant temperature [6, 12-14]. When the aftertreatment system temperature drops, the PCM will cool down and solidify, releasing the stored thermal energy to the catalytic converter substrate [15]. This allows the storage of the exhaust gas thermal energy during the engine's high-load conditions and gradually releases the thermal energy back to the catalyst substrate during the engine-off period. Therefore, the substrate temperature can be kept above the operating limit (i.e. light-off temperature) until the following engine start for improved cold-start emissions' conversion.

The TES system can also moderate the aftertreatment temperature fluctuations during a driving cycle, which can enhance the catalyst's performance and lifespan. Moreover, the use of additives in PCMs improves the thermal conductivity of the PCM and its heat transfer behaviour [12, 15]. Mettawee et al. investigated the benefit of adding aluminium powder to paraffin wax for solar heat storage applications [16]. It was found that embedding aluminium powder into the PCM can lead to a 60% reduction in the charging time of the TES system, as it can significantly enhance the thermal conductivity of the PCM mixture. In a different study, exfoliated graphite nano-platelets (xGnP) were added to paraffin wax to achieve a composite PCM of high latent heat and high thermal conductivity [17]. This resulted in increasing the thermal conductivity of the PCM mixture from approximately 0.25 $W.m^{-1}.K^{-1}$ to 2.41 $W.m^{-1}.K^{-1}$. It was also found

that the latent heat of the paraffin and the thermal stability of the PCM mixture were slightly improved.

TES systems can also be used to accelerate engine oil and coolant warm-up during engine cold-start. Park et al. [18, 19] designed a PCM thermal storage system to recover and recycle the waste heat energy of the coolant system. Implementing this TES system on a 1.6-L diesel engine resulted in roughly 40% reduction in the coolant warm-up time to 95°C and a 2.71% decrease in fuel consumption was reported over the NEDC. Vittorini et al. [20] studied thermal management of engine oil via exhaust gas waste heat recovery to decrease the engine friction and consequently its fuel economy. In this study, fuel consumption, CO and HC emissions were reduced by 3.6%, 7.2% and 3.5%, respectively [20].

M. Gumus tested PCM thermal energy storage systems in gasoline engines to control the cold-start emissions [5]. Burch et al. found that by applying a layer of PCM around a three-way catalyst (TWC) in a gasoline engine, the TES system retained an acceptable level of thermal energy for approximately 24 hours after a driving cycle [21]. This resulted in an 84% reduction in non-methane hydrocarbons (NMHCs) and a 91% reduction in CO emissions when the engine was re-started. Variable conductance vacuum insulation (using metal hydrides) was also used to minimize the heat loss to the atmosphere and also prevent the catalyst from over-heating during the engine's high-load conditions.

Korin et al. investigated different PCM/catalyst layouts to increase the heat transfer between the PCM and the three-way catalyst [22]. His design proved to be effective; however, the catalyst's temperature only remained above its light-off for approximately four hours after the engine's shut-down. This highlights the significance of insulation,

alongside the PCM, in minimizing the heat loss to the atmosphere for improved heat retention capability.

Gaiser et al. experimentally studied a TES system in a sequential arrangement with an SI engine's catalytic converter [23]. This included a heat exchanger to transfer the heat to the exhaust gas, and vacuum insulation for minimizing the heat loss to the atmosphere. Although this arrangement accelerated the catalyst's light-off behaviour, integrating the TES system into the catalyst proved to be substantially more effective. In an integrated TES system arrangement, the catalyst can remain hot during the engine-off periods; whereas in a sequential arrangement, the heat is stored in the upstream device and the catalyst cools down shortly after the engine's shut-down. Therefore, the catalyst needs to light-off again with the aid of the upstream TES system. This can lead to increased emissions compared to the integrated TES system arrangement.

Considering the different nature of diesel exhaust gas aftertreatment in terms of temperatures, gaseous composition and catalysts, a thermal energy storage system has to be developed and investigated based on its requirements. Extensive reviews on the application of PCM have been published by [12, 24-27]; however, there are only a few studies in the field of the application of PCM in compression ignition engines for controlling pollutants.

In this study, a novel PCM thermal energy storage system is developed for light-duty diesel aftertreatment applications for maximum emissions' reduction. This was achieved by investigating different materials for PCM additives and catalyst substrates to improve the thermal behaviour of the TES system.

The aim of this study is to utilize state-of-the-art mechanical, chemical and material engineering sciences to enhance the effectiveness of a thermal energy storage system integrated into a diesel oxidation catalyst. The benefits of this system can be further extended in series hybrid vehicles in which a repetitive engine cold-start is expected. Moreover, by absorbing the excessive heat during the engine's high-load conditions, the catalyst's durability can be improved due to the decreased catalyst active sites sintering and thermal shocks.

2. Methodology

An ANSYS Fluent® model was developed to simulate the PCM behaviour where the thermal energy storage system was integrated into the aftertreatment system. The Exothermia Axisuite® modelling package was used to perform the aftertreatment simulations. The model was created based on a close-coupled full-size DOC and its inlet exhaust gas conditions were extracted from a Euro 5 V6 Jaguar Land Rover research test engine operating on the NEDC. The test engine was equipped with a turbocharger to provide more demanding conditions for the DOC in terms of exhaust gas temperature. The models were calibrated and validated based on the experimental data for maximum consistency.

2.1. Design of the Thermal Energy Storage (TES) System

The TES system can be used both upstream of the catalytic converter to heat up the exhaust gas, or directly integrated into or around the catalyst. In this study, the integrated TES system design was implemented with an annular layer of PCM around the oxidation catalyst (Figure 1). This configuration offers the advantage of instant

emissions' conversion with the engine start, as the catalyst can remain hot during the engine-off periods [23].

In order to select an appropriate PCM for the diesel exhaust gas aftertreatment, a few criteria have to be taken into account. The PCM's melting point should be above the catalyst's light-off temperature, to maintain the catalyst in the operating region while releasing the thermal energy at a constant temperature [14]. At the same time, the PCM's melting point needs to be low enough so that the PCM can liquefy over a driving cycle (e.g. NEDC) for maximum thermal energy storage.

High PCM latent heat of fusion (L) and specific heat capacity (C_p) are other main criteria which can minimize the PCM's mass requirement for packaging purposes. The thermal conductivity (λ) of the PCM can significantly affect the heat transfer rate of the TES system; hence, phase change materials with higher thermal conductivity can respond faster to the transient environment of the exhaust gas aftertreatment.

The catalyst used in this study has a light-off temperature of about 150 °C; therefore, PCMs with a phase change temperature between 170 °C and 200 °C were considered. Comparing the commercially available phase change materials, X180 PCM from PlusICE has been selected and its specifications are listed in Table 1. In the reference model, the TES system consists of 2 kg of PCM salt surrounding the DOC ceramic substrate with a vacuum insulation. Unless otherwise stated, a 10% PCM liquid fraction was assumed as an initial condition at the start of the NEDC to standardise different investigations.

Table 1: Modelled PCM Specifications

PCM Specification	Data
Phase Change Temperature [$°C$]	180
Latent Heat of Fusion [$kJ.kg^{-1}$]	280
Specific Heat Capacity [$kJ.kg^{-1}.K^{-1}$]	1.4
Thermal Conductivity [$W.m^{-1}.K^{-1}$]	0.36

2.2. Selection of PCM, PCM Additives and Catalyst Materials

In order to enhance the heat transfer between the PCM and the catalyst, the application of mixing additives to the PCM was investigated. This can lead to an increase in the thermal conductivity of the PCM-additive mixture, to improve the TES system's response time to the transient environment of the aftertreatment system. In conjunction with the PCM additives, the effect of the catalyst's substrate material on the thermal energy transfer from the PCM to the catalyst's active sites was also investigated.

Aluminium, copper and graphite were selected, based on the exhaust gas aftertreatment requirements, from the studied PCM additive materials in the literature [16, 28]; their properties are listed in Table 2. These additives were mixed with the PCM salt by 10% mass ratio. Assuming a homogeneous mixture, the PCM-additive mixtures' properties are calculated based on Equations 1 to 3 and are summarized in Table 3. Adding 10% graphite to the PCM leads to a 26 times increase in the PCM-additive mixture's thermal conductivity from $0.36 W.m^{-1}.K^{-1}$ to $9.46 W.m^{-1}.K^{-1}$. The mixture's latent

heat decreases by 10% as the additive portion of the mixture is not able to change its phase at the same temperature as the PCM.

Table 2: PCM Additive Materials' Properties

Material Properties	Aluminium	Copper	Graphite
Density [$kg.m^{-3}$]	2700	8960	2200
Thermal Conductivity [$W.m^{-1}.K^{-1}$]	160	390	145
Specific Heat [$J.kg^{-1}.K^{-1}$]	950	380	710
Melting Point [$°C$]	620	990	3800

$$\boldsymbol{\rho_{Mixture} = \rho_{PCM} v_{f,PCM} + \rho_{Additive} v_{f,Additive}} \quad \text{Equation 1}$$

$$\boldsymbol{\lambda_{Mixture} = \lambda_{PCM} v_{f,PCM} + \lambda_{Additive} v_{f,Additive}} \quad \text{Equation 2}$$

$$\boldsymbol{C_{p,Mixture} = C_{p,PCM} m_{f,PCM} + C_{p,Additive} m_{f,Additive}} \quad \text{Equation 3}$$

where ρ is density; $\vec{v}$ is fluid velocity; λ is thermal conductivity; C_p is specific heat capacity.

Table 3: PCM Additive Mixtures' (10% by Mass) Properties

Mixture Properties	PCM	PCM Aluminium Mixture	PCM Copper Mixture	PCM Graphite Mixture
Density [$kg.m^{-3}$]	1330	1401	1454	1385
Thermal Conductivity [$W.m^{-1}.K^{-1}$]	0.36	8.64	6.68	9.46
Specific Heat [$J.kg^{-1}.K^{-1}$]	1400	1355	1298	1331

Latent Heat [$kJ.kg^{-1}$]	280	252	252	252

In this study catalyst substrates made of ceramic and metallic materials have also been investigated. Comparable ceramic and metallic substrates with a cell density of 400 *cpsi* were selected and their specifications are listed in Table 4. The metallic substrates' thermal conductivity is approximately 10 times higher in comparison to the ceramic substrate. This can lead to a higher heat transfer rate and more uniform temperature contours over the catalyst's substrate. Although the specific heat of the metallic substrate is lower, the substrate's thermal inertia is slightly higher due to its increased mass.

Table 4: Ceramic and Metallic Substrates' Specifications

Specifications	Ceramic Substrate	Metallic Substrate
Wall Thickness [*Mil*]	4	3
Density [$kg.m^{-3}$]	2092	7900
Thermal Conductivity [$W.m^{-1}.K^{-1}$]	1.5	14.5
Specific Heat [$J.kg^{-1}.K^{-1}$]	930	431

2.3. ANSYS Fluent® PCM Modelling

To investigate the effect of a phase change material (PCM) thermal energy storage system on the diesel aftertreatment, a transient CFD model was developed using the ANSYS Fluent® 15 CFD package. The model can simulate PCM solidification and melting

over a driving cycle. It can also predict the PCM's cooling behaviour for a prolonged period of time after vehicle shut down, where the thermal energy storage system can maintain the catalyst in an operational temperature window. To estimate the thermal effect of the PCM on the DOC, the heat transfer rate between the catalyst and the PCM was extracted from this model and imported into the Axisuite model. Both Axisuite and ANSYS Fluent models share similar attributes and assumptions unless otherwise stated.

2.3.1. Model Geometry and Boundary Conditions

As schematically illustrated in Figure 1, the model's geometry is based on a close-coupled full-size DOC substrate with a thermal energy storage system integrated into the catalyst canning. There are 2 kg of PCM salt encapsulated in a metallic annulus with a wall thickness of 2 mm surrounding the catalyst's external periphery. Since the thermal energy storage system needs advanced insulation for maximum heat retention, vacuum insulation was introduced for the canning's external wall.

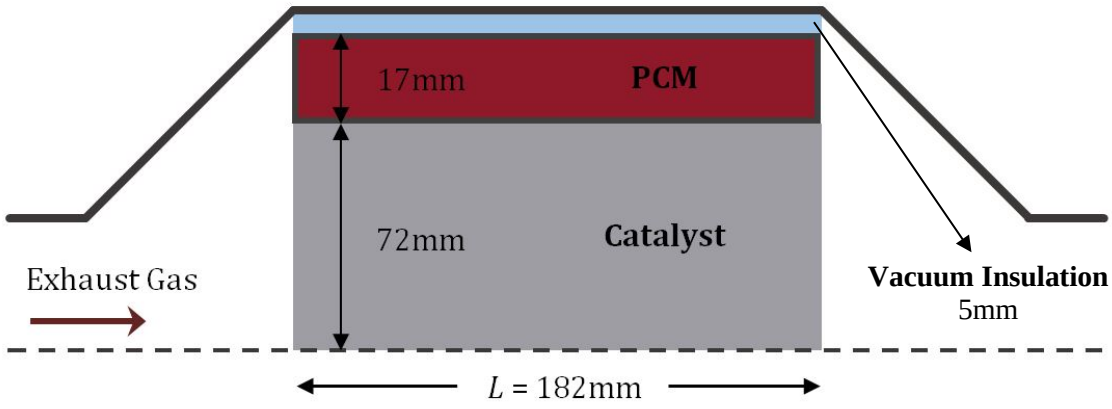

Figure 1: PCM Model Geometry Diagram

To simulate the model's inlet exhaust gas conditions, a user defined function (UDF) was developed in C programming language. As shown in Figure 2, this included an array

of the exhaust gas inlet temperature and mass flow rate for each time step of the NEDC, based on experimental data. The ambient temperature and air pressure were assumed to be 25 °C and 101 kPa, respectively. Once the driving cycle has finished after 1200 seconds, the UDF assigns ambient conditions to the system inlet and outlet to simulate the engine-off period.

The catalyst in an aftertreatment system has a dense honeycomb design that would require complicated geometry and mesh to represent it. In this study, the catalyst was assumed to be porous media with high viscosity and radial inertial forces to represent the substrate channels [29].

The model's geometry was discretized to an axisymmetric 2D structured grid with different zones for the inlet, catalyst, PCM and outlet. The boundaries between the different zones were defined as mesh interfaces to facilitate mass and heat transfer between zones as required. To ensure that the results are grid-independent, the mesh was gradually refined to achieve a maximum of 0.5% difference in the system's outlet temperature value.

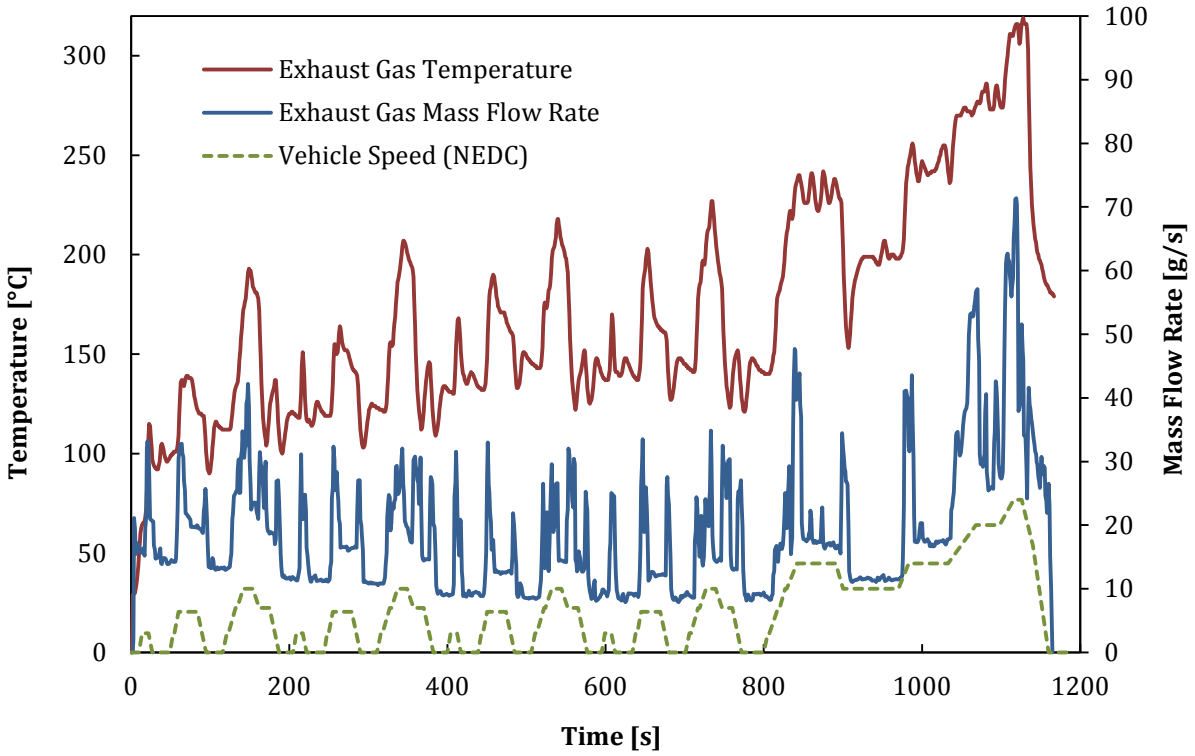

Figure 2: Exhaust Gas Temperature and Mass Flow Rate at the System Inlet

2.3.2. Modelling Theory and Governing Equations

The model's theory is based on physical conservation laws and it employs a finite volume method. The simulation was set to be transient with a time step of one second and uses the coupled pressure-based solver. The standard k-ε turbulence model was used for the inlet and outlet zones; while flow was assumed to be laminar (based on the calculation for Reynold number ≅ 225) in the porous catalyst zone due to high viscous forces, as Reynold number was calculated

The solidification/melting model was used to simulate the phase change of the PCM. Although a solid-solid PCM was chosen, the model is still applicable as the latent heat energy can be simulated, neglecting the actual phase of the material. This model uses the latent heat capacity of the PCM to predict the amount of energy which is absorbed

during melting, or released during solidification phases. The energy balance equation for calculating the heat conduction in this model is defined as:

$$\frac{\partial}{\partial t}(\boldsymbol{\rho H}) + \boldsymbol{\nabla}.(\boldsymbol{\rho}\vec{\boldsymbol{v}}\boldsymbol{H}) = \boldsymbol{\nabla}.(\boldsymbol{\lambda}\boldsymbol{\nabla T}) + \boldsymbol{S} \qquad \text{Equation 4}$$

The enthalpy H is calculated as follows:

$$\boldsymbol{H} = \boldsymbol{h} + \Delta\boldsymbol{H} \qquad \text{Equation 5}$$

The latent heat content ΔH which is defined as:

$$\Delta\boldsymbol{H} = \boldsymbol{\beta L} \qquad \text{Equation 6}$$

where ρ is density; $\vec{v}$ is fluid velocity; λ is thermal conductivity; S is source term; h is the sensible enthalpy; β is the liquid fraction; and L is the latent heat of the material.

The temperature of the PCM between the solidus and liquidus temperatures defines the liquid fraction; when at 0 the PCM is fully solid and at 1 it is fully liquid. In this model, a temperature range of 2 °C is used to simulate the phase change region of the PCM. The initial PCM temperature is set during the model's initialisation step to reproduce a hot-start if required.

2.3.3. Model Calibration and Validation

The model was calibrated for both the catalyst's outlet exhaust gas temperature and pressure drop. This was achieved by modifying the properties of the porous media: including the porosity, viscosity and inertial resistances. To ensure consistency, the calibrated model was compared with a set of reference data for validation purposes, as shown in Figure 3. Inlet exhaust gas temperature (T Gas) was provided as an indicator of exhaust manifold conditions over the NEDC. The model slightly underestimates the

catalyst's outlet temperature; which can be caused by the catalyst's porous media assumption in which increased heat transfer rate and consequent heat loss to the atmosphere are expected.

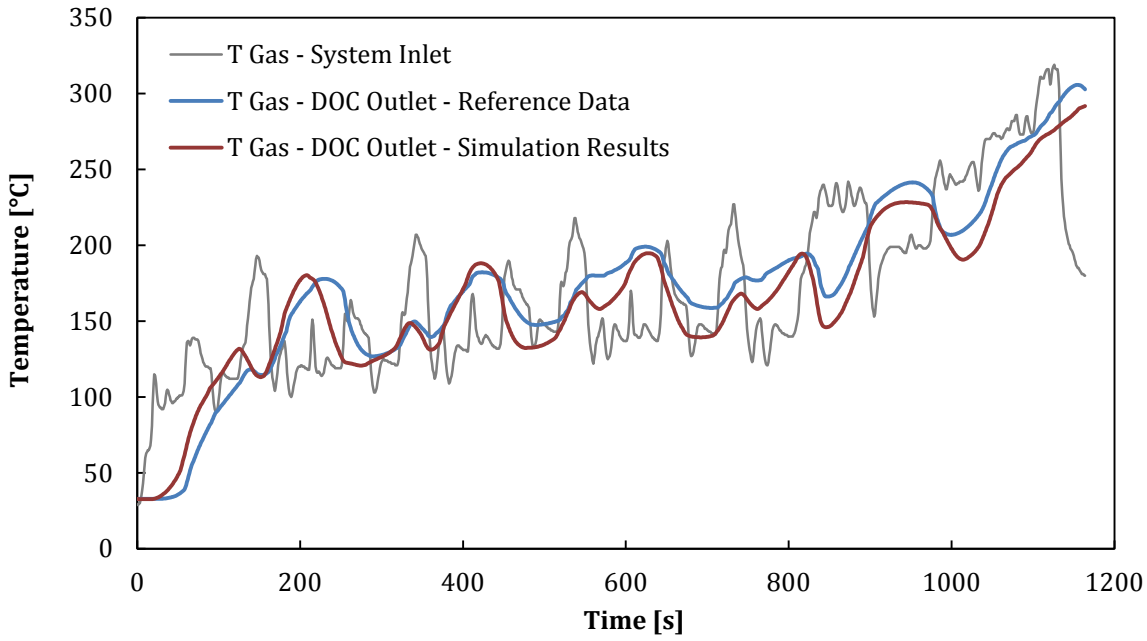

Figure 3: ANSYS Fluent Model Validation

2.4. Exothermia Axisuite® Aftertreatment Modelling

In the present study, aftertreatment chemical reactions were simulated in the commercial Exothermia Axisuite® package. This software is able to model the transient behaviour of aftertreatment components including flow-through catalysts and predict their time-based temperature profiles and exhaust gas composition. To investigate the effect of the TES system on the emissions reduction performance of the DOC, an Axisuite model was developed. This model has similar geometry, boundary conditions and assumptions as discussed in Section 2.3.1. Axisuite standard DOC chemical reactions scheme was used to simulate the chemical reactions occurring over the DOC. The full

methodology and detailed characteristics of the model are explained by Lafossas et al. [30].

To simulate the chemical reactions occurring over the DOC, the molar fractions of N_2, O_2, CO_2, H_2O, CO and HC species of the inlet exhaust mixture for each time step of NEDC were extracted from experimental data. This model can predict the rate and enthalpies of CO and THC oxidation reactions, based on their species' concentration, exhaust gas temperature and pressure. Also, the principle of the model's creation for simulation was explained in the author's previous paper in which thermal performance of diesel aftertreatment was investigated in the Exothermia Axisuite® package [3]. The DOC model was validated by comparison with experimental data from a diesel engine provided by Jaguar Land Rover for the purpose of this research study. As shown in Figure 4, adequate consistency with experimental data was found in the simulated results of cumulative CO and THC emissions over the NEDC.

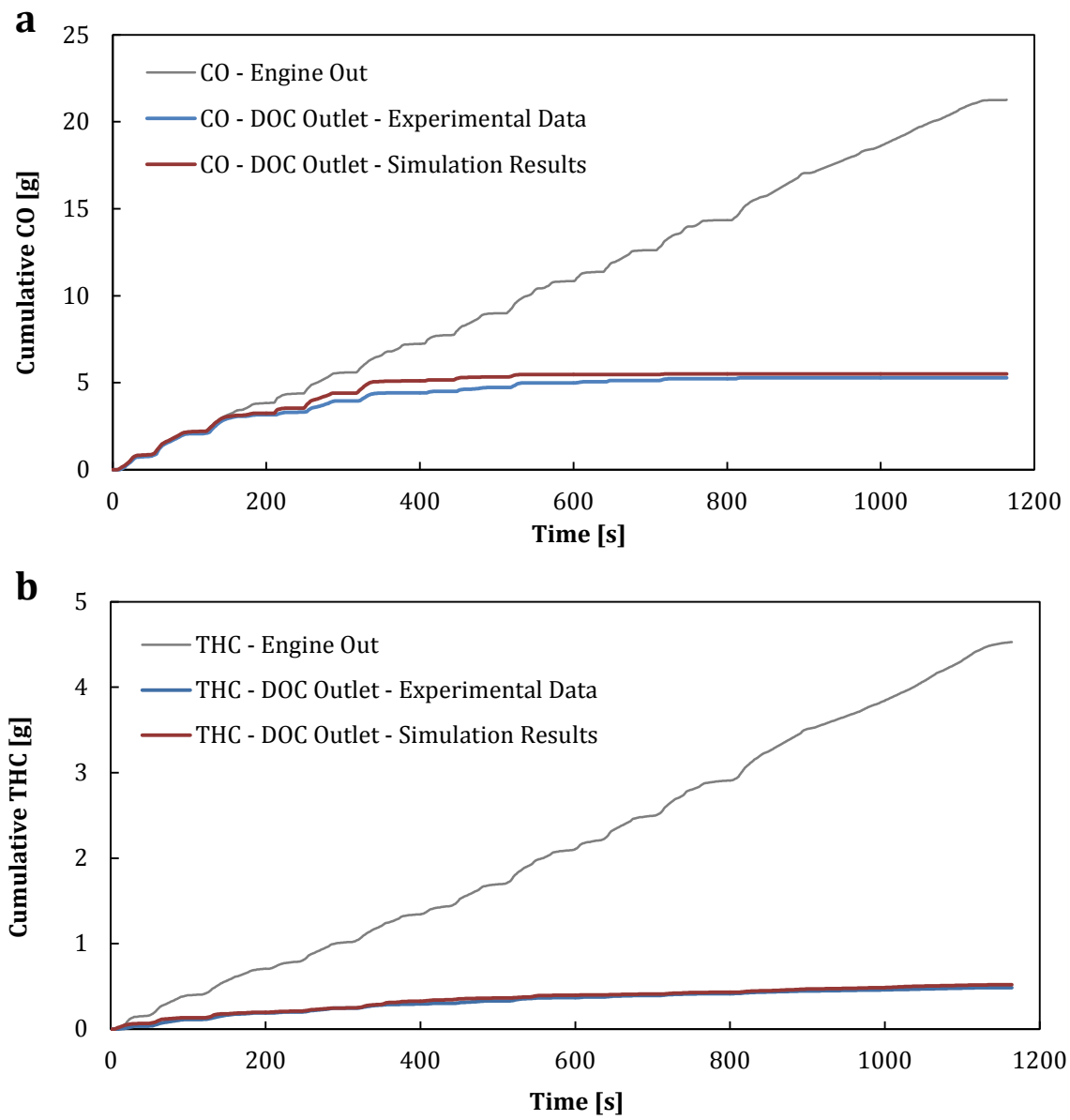

Figure 4: Axisuite Model Validation (a) Cumulative CO Emissions; (b) Cumulative THC Emissions

3. Results and Discussion

3.1 Preliminary Study

The aftertreatment temperature profiles of the reference model are shown in Figure 5. The results indicate that when the DOC is equipped with a TES system, the

DOC outlet temperature would start at the initial temperature of the PCM (180 °C), and it increases by about 12 °C during the first 60 seconds of the NEDC. This temperature increase is mainly associated with the exothermic oxidation reactions over the DOC. As shown in Figure 6(a) and Figure 6(b), almost complete conversion of CO and THC emissions were achieved during this period.

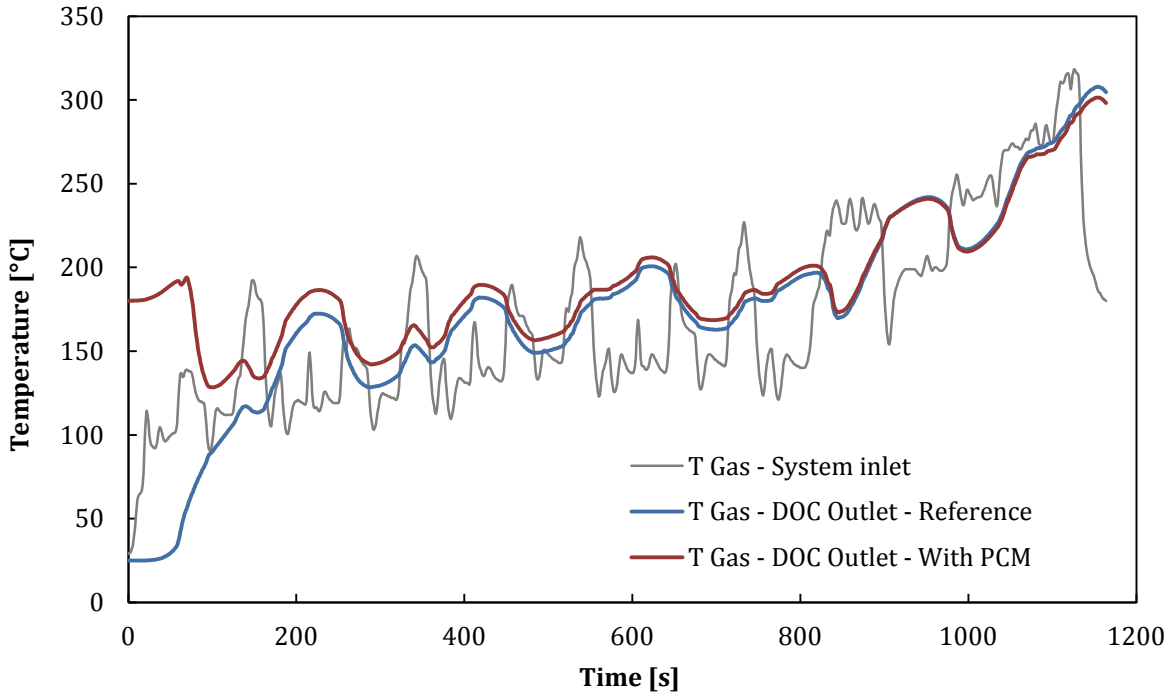

Figure 5: PCM Reference Model Temperature Profiles

Following this increase, a sharp decrease of around 62 °C in the DOC outlet temperature was observed over the subsequent 30 seconds of the NEDC. During this period, the TES system is no longer able to provide enough heat to the catalyst and relatively cold passing exhaust gas tends to cool down the catalyst abruptly. As shown in Figure 6(a) and Figure 6(b), this temperature drop leads to catalyst light-out and a subsequent reduction in the emissions' conversion performance.

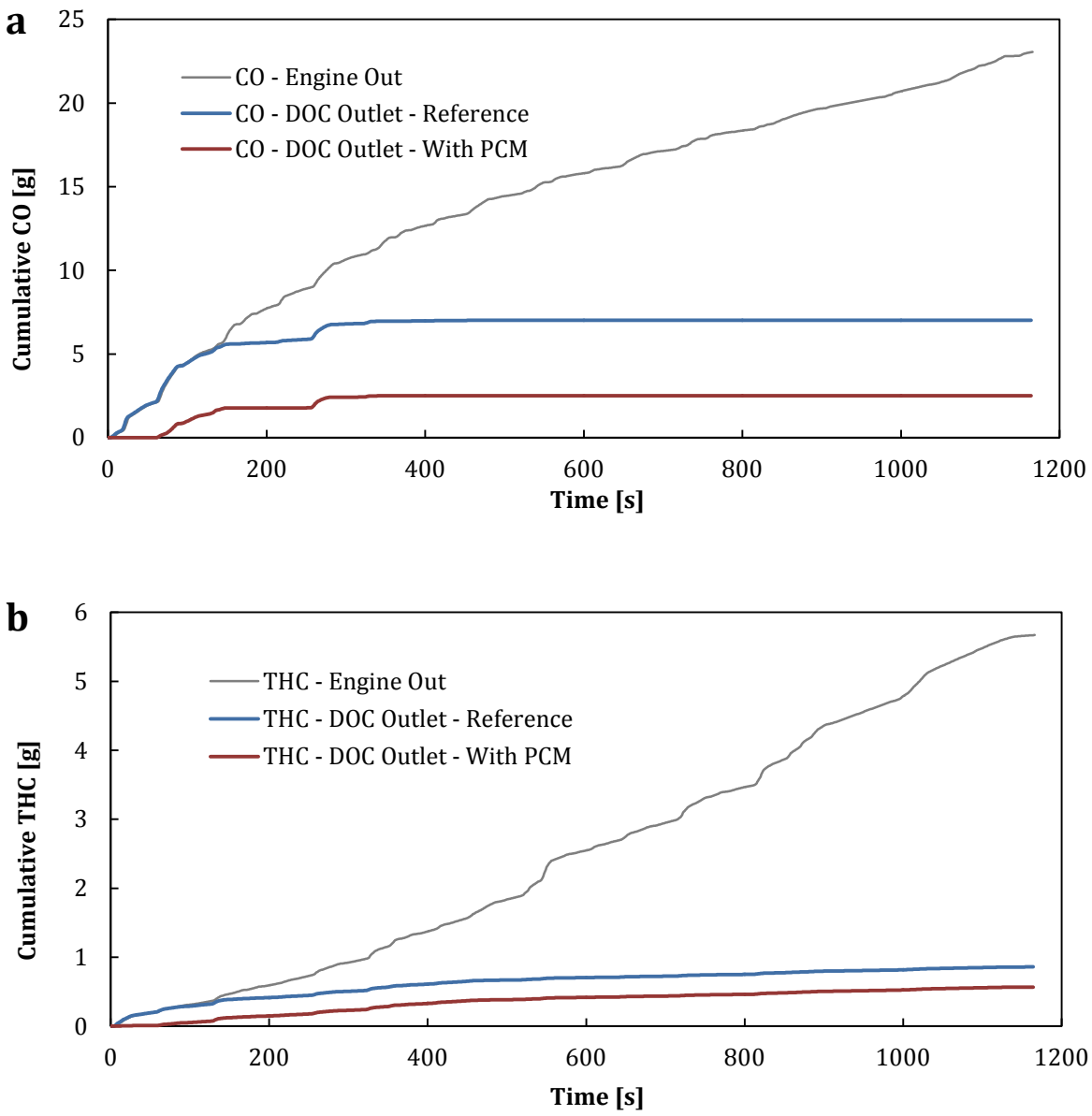

Figure 6: Effect of the TES System on the Vehicle's Cumulative CO Emissions (a); THC Emissions (b)

For the rest of the NEDC urban cycle, the TES system results in approximately a 9 °C temperature increase in comparison to the reference case without PCM, as shown in Figure 5. However, during the extra-urban cycle of the NEDC, the TES system decreases the catalyst outlet's temperature slightly as it absorbs the excessive heat. In terms of

emissions' conversion, results indicated that this TES system design can decrease the CO emissions by 64% and THC emissions by 34% over the NEDC.

3.2 PCM Additives' and Catalyst Substrate Materials' Effect

The thermal behaviour of the TES system with the PCM-graphite mixture and metallic substrate was extracted from the ANSYS Fluent model and compared to the reference case. This includes the PCM's liquid fraction (Figure 7(a)), the PCM's internal energy (Figure 7(b)) and heat flux from the PCM's wall to the catalyst (Figure 7(c)). As discussed previously, adding 10% graphite to the PCM salt decreases the initial PCM internal energy as the additive is not able to change its phase and store the thermal energy.

Figure 7(a) illustrates that the PCM in the reference case gradually solidifies and releases its stored thermal energy over the urban part of the NEDC, as its liquid fraction decreases from 0.10 to around 0.02. During the extra-urban cycle of the NEDC the PCM melts and increases its liquid fraction to 0.11. The metallic substrate proves to behave similarly with slightly improved heat transfer, particularly when storing heat during the extra-urban cycle.

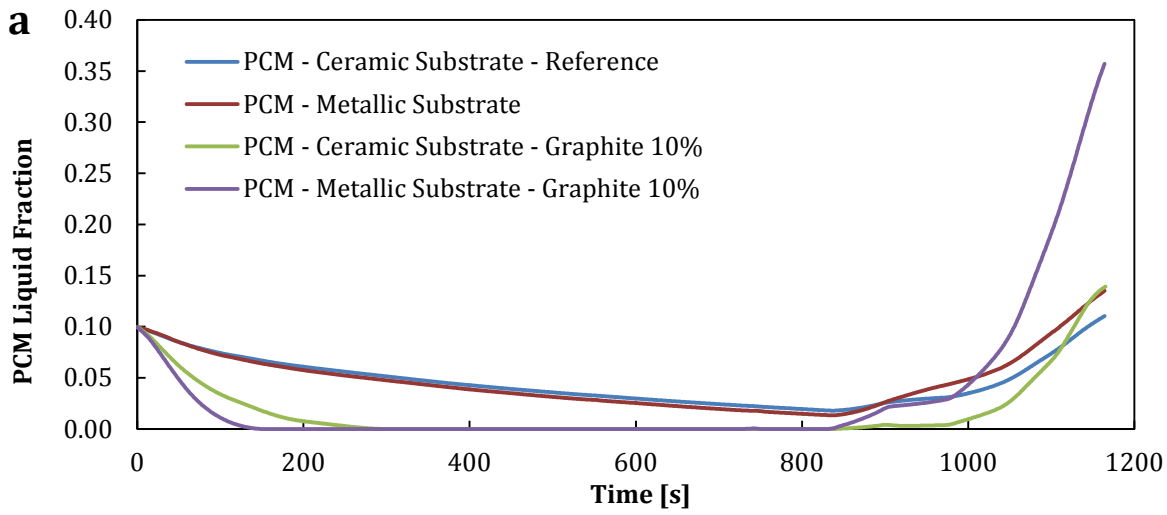
a
PCM Liquid Fraction
0.40
0.35
0.30
0.25
0.20
0.15
0.10
0.05
0.00
0
200
400
600
800
1000
1200
Time [s]
PCM - Ceramic Substrate - Reference
PCM - Metallic Substrate
PCM - Ceramic Substrate - Graphite 10%
PCM - Metallic Substrate - Graphite 10%

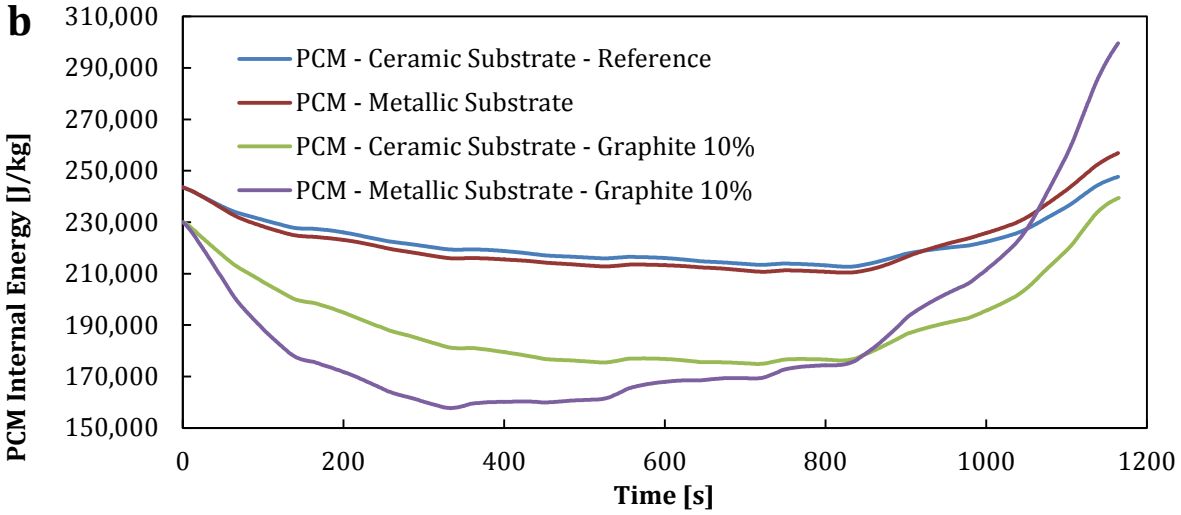
b
PCM Internal Energy [J/kg]
310,000
290,000
270,000
250,000
230,000
210,000
190,000
170,000
150,000
0
200
400
600
800
1000
1200
Time [s]
PCM - Ceramic Substrate - Reference
PCM - Metallic Substrate
PCM - Ceramic Substrate - Graphite 10%
PCM - Metallic Substrate - Graphite 10%

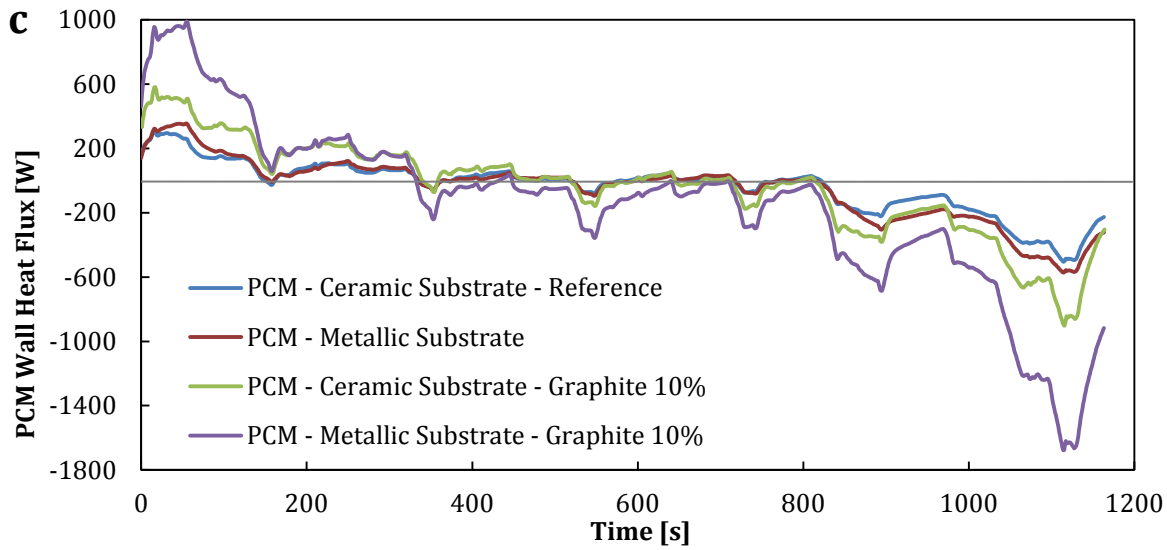
c
PCM Wall Heat Flux [W]
1000
600
200
-200
-600
-1000
-1400
-1800
0
200
400
600
800
1000
1200
Time [s]
PCM - Ceramic Substrate - Reference
PCM - Metallic Substrate
PCM - Ceramic Substrate - Graphite 10%
PCM - Metallic Substrate - Graphite 10%

Figure 7: PCM Additive and Substrate Materials' Effect on the: (a) PCM's Liquid Fraction; (b) PCM's Internal Energy; (c) PCM's Heat Flux to the Catalyst

As shown in Figures 7(a) to Figure 7(c), the graphite additive can considerably increase the PCM's performance in releasing and storing thermal energy. The results indicate that 10% graphite can increase the PCM's heat discharge rate by 121% during the first 200 seconds of the NEDC; while 71% more thermal energy was absorbed during the NEDC's extra-urban cycle.

Using a metallic substrate in conjunction with the PCM graphite mixture leads to further improvement in the TES's thermal performance, particularly where there is a high temperature gradient between the exhaust gas and the PCM (e.g. cold-start). As illustrated in Figure 7(a), this combination can assist the PCM to completely discharge its stored latent heat during the first 150 seconds of the NEDC, when the DOC demands a high level of thermal energy to remain activated for emissions' conversion.

Moreover, the metallic substrate significantly helps the PCM graphite mixture to melt and store more thermal energy throughout the NEDC's extra-urban cycle. As shown in Figure 7(a), the PCM liquid fraction can reach up to 0.36 over the extra-urban cycle, with the metallic substrate and graphite additive; while a PCM liquid fraction of 0.14 was achieved in the reference case. It should be noted that the NEDC is a comparatively low-load driving cycle, in which the thermal energy available for the PCM to store is limited.

Considering the results, it can be concluded that the PCM's thermal energy is relatively confined within the PCM due to its low thermal conductivity. Consequently, the thermal energy is not able to transfer to the catalyst's substrate in a timely manner,

as required by the exhaust aftertreatment system. Furthermore, low thermal conductivity of the catalyst's substrate can limit the heat penetration into the core of the catalyst and its active sites, where most of the emissions' conversion reactions occur. Therefore, alleviating these two issues with the PCM graphite additive and metallic substrate turns out to significantly improve the TES system performance.

Figure 8 illustrates the ceramic and metallic DOCs' temperature profiles with and without the TES system. The metallic DOC tends to heat up more gradually compared to the ceramic DOC, due to its higher thermal inertia as discussed previously. Moreover, its temperature profile shows lower fluctuations as higher thermal conductivity of the metallic substrate leads to a more uniform heat distribution over the catalyst's substrate during a driving cycle. Results indicate similar behaviour when comparing the ceramic and metallic DOCs equipped with the TES system as well.

As discussed previously, the TES system with the PCM-graphite mixture and metallic substrate can enhance utilization of the PCM's thermal energy storage capacity. This effect is shown in Figure 8, as the local maximum temperature was elevated by 68 °C to 209 °C at 87 seconds after the cold-start, due to the improved heat transfer and promoted oxidation reactions. Following this peak, the drop in the DOC's outlet temperature diminished considerably (from 62 °C to 49 °C) and the DOC outlet temperature reached its local minimum of 160°C at 172 seconds after the cold-start.

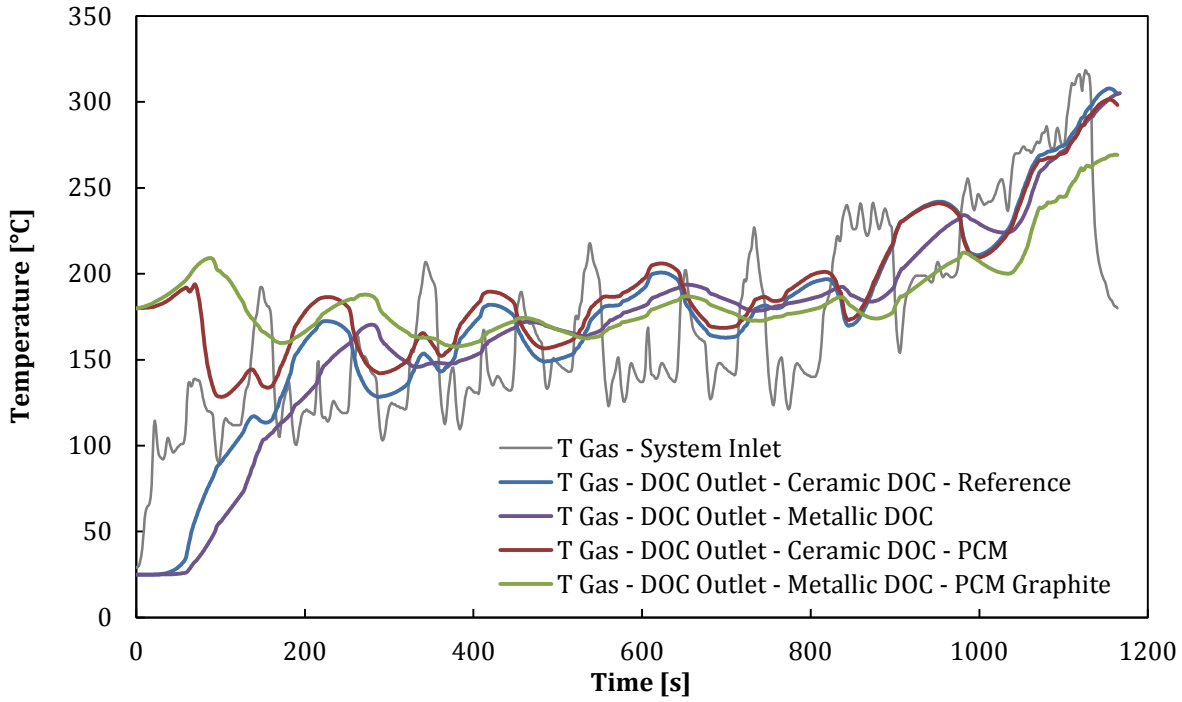

Figure 8: PCM Additive and Substrate Materials' Effect on the DOC's Temperature Profiles

Considering the extra-urban cycle of the NEDC in Figure 8, the improved TES system reduces the average DOC outlet temperature from 235 °C to 210 °C; while the baseline TES system reduces it to 229 °C. In more aggressive driving cycles, this temperature drop can result in improved durability and extend the catalyst's operational life. It should be also noted that the improved TES system maintains the DOC outlet temperature above 157 °C over the NEDC, which is above the catalyst's light-off temperature.

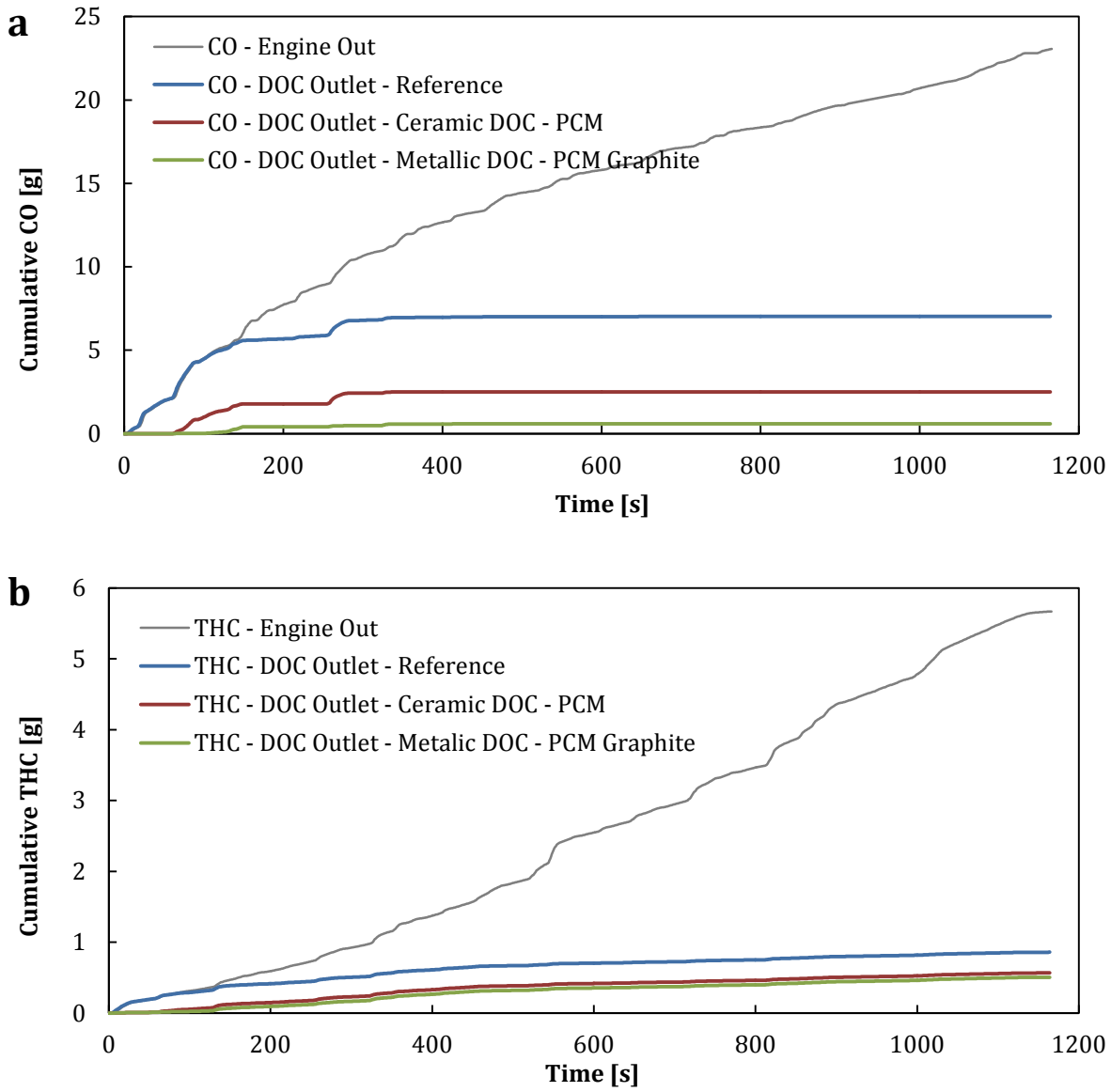

Figure 9: PCM Additive and Substrate Materials' Effect on the Vehicle's Cumulative CO Emissions (a); THC Emissions (b)

Figure 9(a) illustrates the effect of the PCM additive and substrate material on the vehicle's cumulative CO emissions. The PCM-graphite mixture in conjunction with the metallic substrate proves to reduce the cumulative CO emissions by 91.7%, as described in Table 5. The DOC tends to slightly light-out at around 137 seconds after the cold-start. At this point, the TES system is not able to provide enough thermal energy to the catalyst, since most of its stored latent heat has been already discharged (Figure 7(a)).

Table 5: Summary of PCM Additive and Substrate Materials' Effect on the Vehicle's Emissions

Case	Cumulative CO (g)	CO Emissions' Reduction (%)	Cumulative THC (g)	THC Emissions' Reduction (%)
Ceramic DOC - No PCM (Reference)	7.02	-	0.859	-
Ceramic DOC - PCM	2.50	64.4	0.567	34.0
Metallic DOC - PCM Graphite	0.58	91.7	0.505	41.2

As shown in Figure 9(b) and listed in Table 5, the improved TES system can increase the THC emissions' conversion by 41.2% compared to the reference case. Hydrocarbon speciation results indicate that 88% of the emitted THC in the improved TES system is methane (CH_4). The C-H bonds in methane are exceptionally stable (with a bond energy of 435 kJ/mol) compared to other alkane hydrocarbons [31]. Therefore, sufficient methane oxidation over conventional catalysts requires considerably higher temperatures, which are challenging to achieve in diesel exhaust gas aftertreatment during the NEDC.

3.3 TES System Cooling

In this section the cooling behaviour of the improved TES system has been investigated to evaluate its thermal energy retention capability. During the engine-off periods, the aftertreatment system was assumed to be at the atmospheric temperature of 25 °C and without any input from the engine for modelling purposes. It was also assumed that the aftertreatment and TES systems start the cooling procedure at the melting temperature of the PCM (180 °C) and with the PCM completely melted (liquid

fraction of 1). The TES system's insulation and PCM's mass can significantly affect the TES's thermal energy retention capability and its cooling behaviour. Therefore, vacuum insulation was taken into account and PCM mixture masses of 1, 2 and 3 kg were investigated.

As shown in Figure 10(a), each kilogram of the PCM mixture requires approximately 4 hours and 56 minutes to completely solidify. During this period, the PCM releases its stored thermal energy and maintains the aftertreatment system temperature at around 180 °C (Figure 7(b)). Since this is an isothermal (constant temperature) process, the heat transfer rate remains constant and the PCM liquid fraction declines linearly with respect to time.

Following the PCM's complete solidification, the catalyst's average temperature starts to drop and reaches 150 °C in approximately 3 hours for a TES system with 2 kg of PCM mixture. Figure 10(b) shows that the catalyst's cooling rate after the PCM solidification is considerably lower compared to the reference case, due to the improved insulation and added thermal inertia of the PCM.

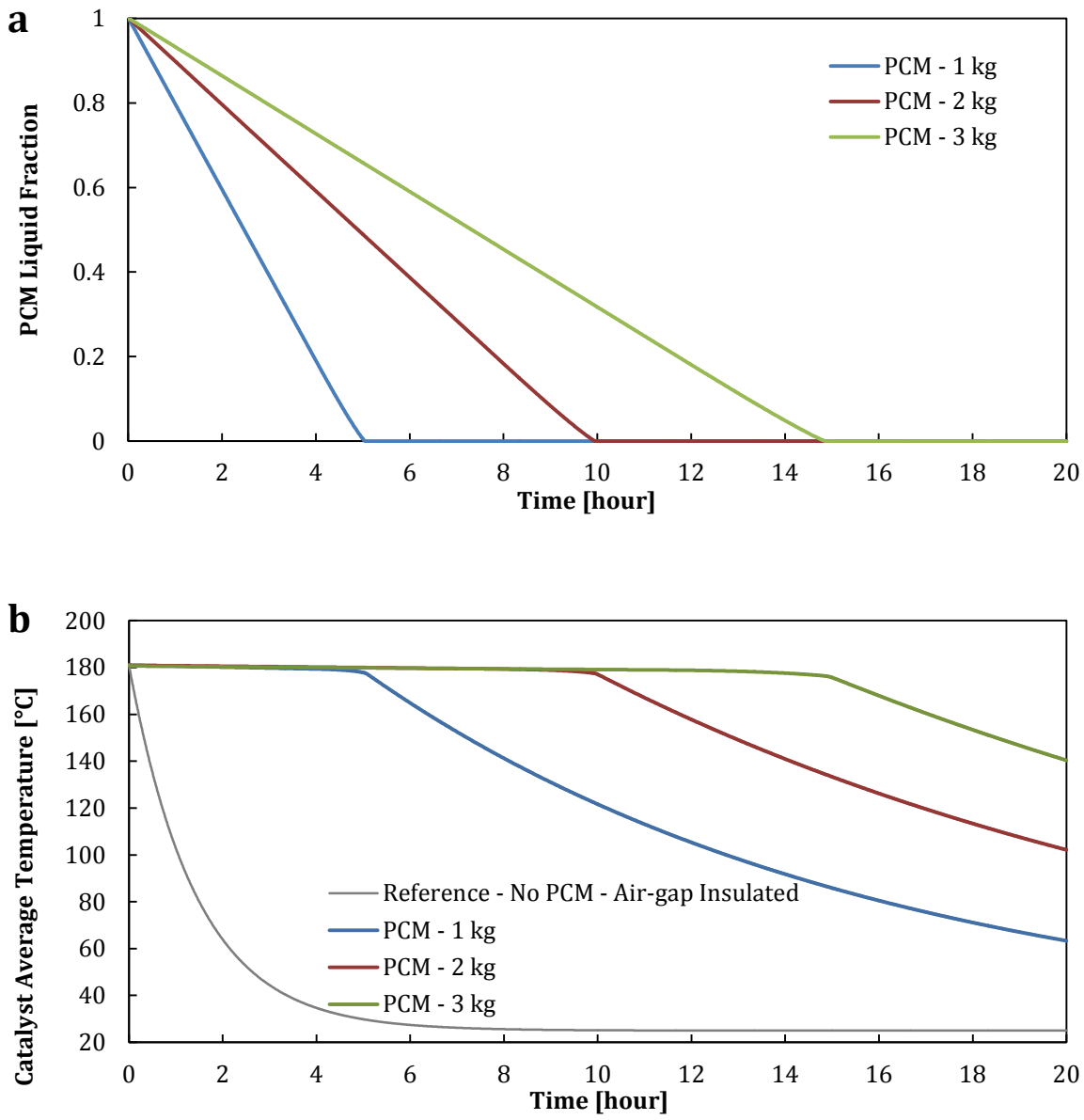

Figure 10: TES System Cooling Effect on the: (a) PCM's Liquid Fraction; (b) Catalyst's Average Temperature

The TES system's 'effective cooling time' was defined as the time required for the fully melted PCM to reach a liquid fraction of 0.1 at atmospheric conditions. As pointed out previously, a PCM liquid fraction of 0.1 was assumed as the model's initial condition for investigating the performance of the TES system. The time needed for the catalyst to cool down to 150 °C has also been included in Table 6. However, as the PCM loses its

energy and its temperature declines, the TES system's effectiveness will deteriorate considerably. It should be noted that in an aggressive or extended driving cycle the PCM can completely melt and its temperature can increase (further than 180 °C), while it is storing excessive exhaust gas thermal energy.

Table 6: TES System Cooling Times for a Varying PCM Mixture's Mass

PCM Mixture Mass	Effective Cooling Time [h:m]	Cooling Time to 150 °C [h:m]
1 kg	4:27	7:13
2 kg	8:49	12:53
3 kg	13:12	18:30

Results indicate that the effective cooling time of 1 kg of PCM mixture is 4 hours and 27 minutes; while it can maintain the catalyst's average temperature above 150 °C for more than 7 hours (Table 6). It can be concluded that increasing the PCM mixture mass by 1 kg can result in prolonging the TES system's effective cooling period by approximately 4 hours and 25 minutes. The maximum thermal energy retention was recorded for the case with 3 kg of PCM mixture; which yielded more than 13 hours of an effective cooling period and maintained the catalyst above its light-off temperature for more than 18 hours.

3.4 Cold-PCM-start and Hot-PCM-start Trade-off

As the PCM cools down to atmospheric temperature and loses its stored thermal energy, its added thermal inertia can act as a heat sink and absorb the heat required for

the catalyst to activate the emissions' conversion reactions. In this section, the trade-off between the effect of a cold and a hot PCM was investigated, to provide more insight into the costs and benefits of a TES system in exhaust gas aftertreatment. The TES system in this study consists of 2 kg of PCM-graphite mixture and metallic substrate as introduced previously.

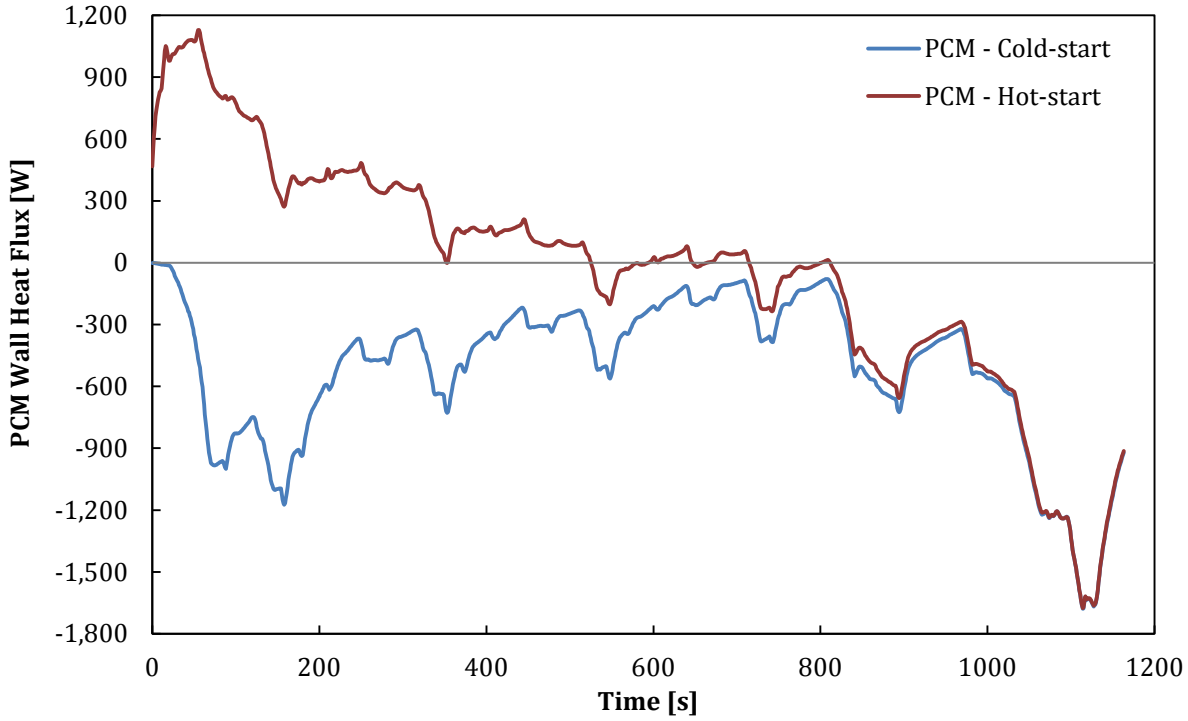

Figure 11: PCM Hot and Cold-Start Effect on the Heat Transfer to the Catalyst

The 'cold-PCM-start' was defined as a condition where the aftertreatment and the TES systems are at an atmospheric temperature (25 °C) at the start of the driving cycle. On the other hand, in the 'hot-PCM-start' condition, it was assumed that the whole aftertreatment system was repeating the NEDC for the second time consecutively. In other words, the initial aftertreatment conditions of the hot-PCM-start case correspond to the final state of the cold-PCM-start case.

As shown in Figure 11, the improved TES system absorbs thermal energy from the catalyst at an average rate of 413 W during the urban part of the NEDC in the cold-PCM-start condition. This increases the PCM-graphite mixture's temperature; however, as illustrated in Figure 12, the PCM remains completely solid during this period.

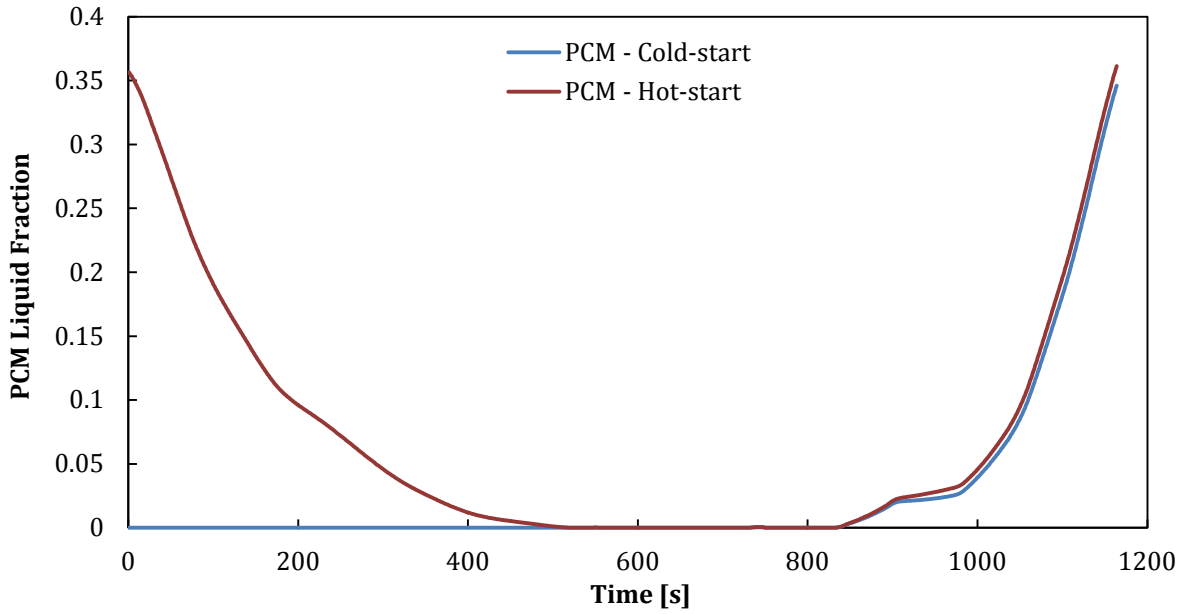

Figure 12: PCM Hot and Cold-Start Effect on the PCM's Liquid Fraction

On the other hand, the TES system in the hot-PCM-start condition can provide thermal energy to the catalyst with an average rate of 261 W during the urban part of the NEDC. As shown in Figure 11, the heat transfer rate is more biased towards the beginning of the driving cycle; this is mainly due to the greater temperature gradients between the PCM and the exhaust gas. Similar thermal behaviour was observed during the extra-urban part of the NEDC, when comparing the cold and hot-PCM-start conditions.

Due to the added thermal inertia of the TES system, the cold-PCM-start condition can significantly reduce the DOC's outlet temperature, particularly during the urban

part of the NEDC (Figure 13). This can result in a 26% increase in CO emissions and a 20% increase in THC emissions compared to the reference case (Figure 14(a) and Figure 14(b)). Considering the hot-PCM-start condition, the stored thermal energy in the PCM helps to maintain the DOC's outlet temperature above 166 °C throughout the NEDC. The results indicate that a 92% reduction in CO emissions and a 42% reduction in THC emissions can be achieved in the hot-PCM-start condition compared to the reference case.

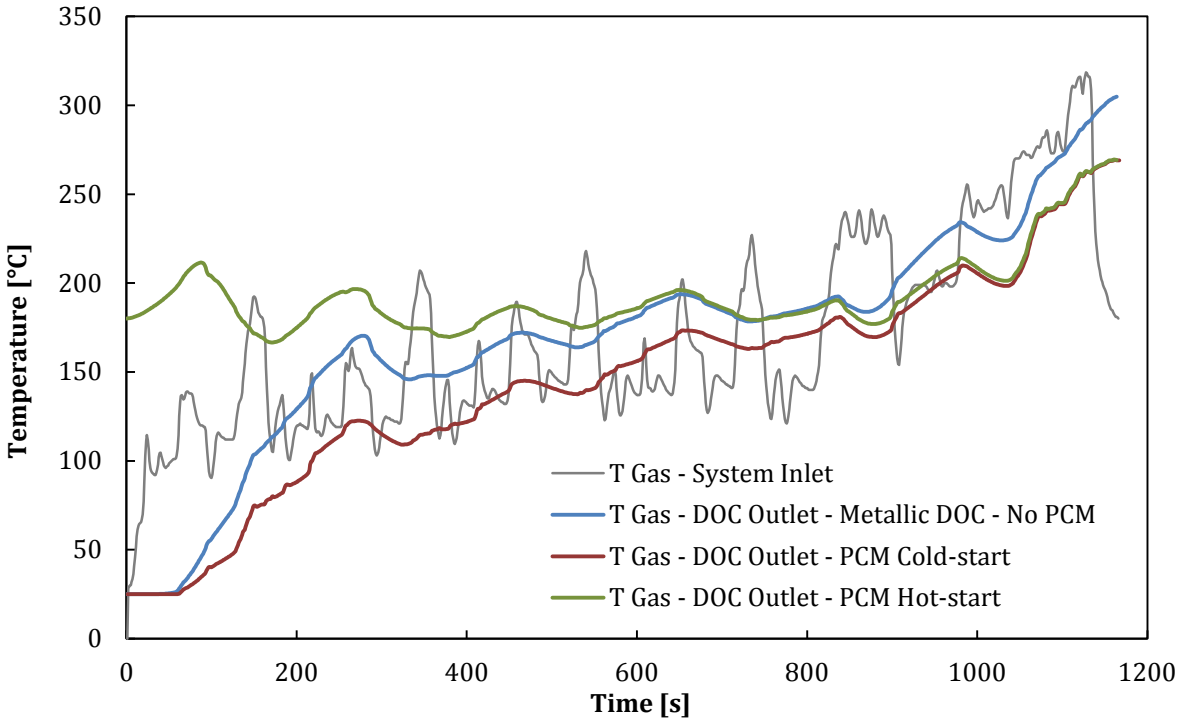

Figure 13: PCM Hot and Cold-Start Effect on the DOC's Temperature Profiles

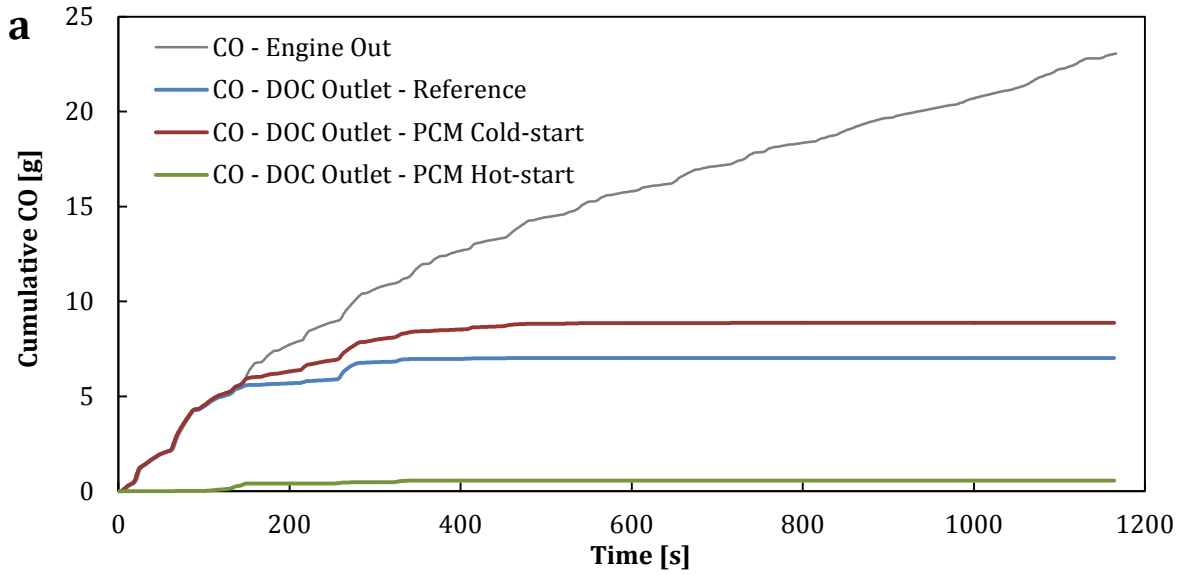

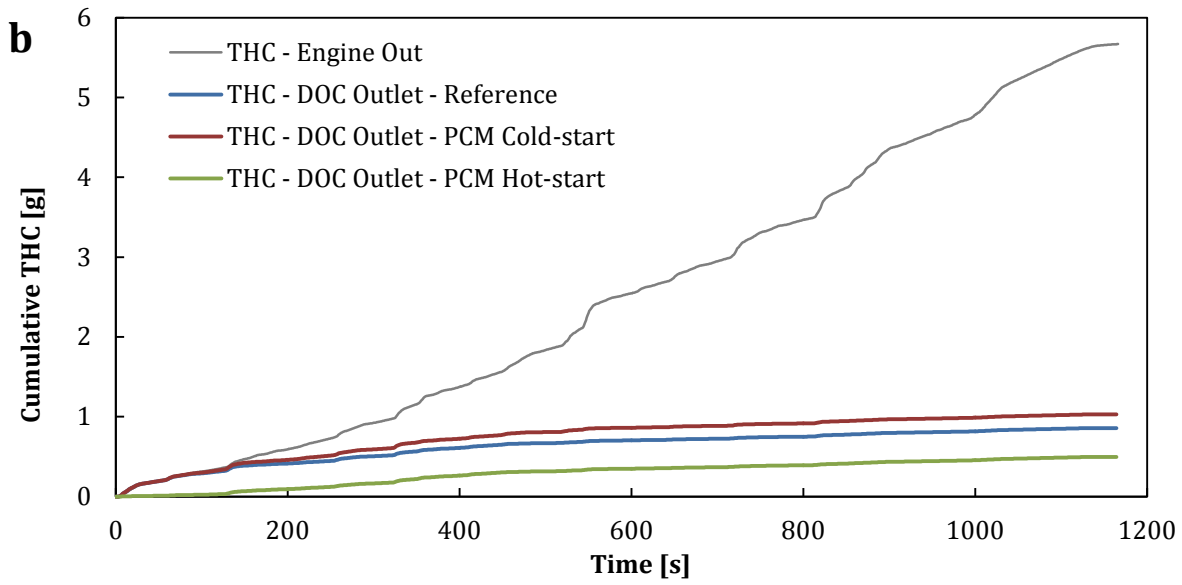

Figure 14: PCM Hot and Cold-Start Effect on the Vehicle's: (a) Cumulative CO Emissions; (b) Cumulative THC Emissions

3.5 TES System Design Optimization Study

In order to further improve the heat transfer rate between the PCM and the catalyst, the TES system design was optimized. As shown in Figure 15, the optimized design features a PCM annulus which accommodates a catalyst core inside and also is surrounded by an annular catalyst. This allows the PCM to transfer thermal energy to the catalysts by its inner and outer surfaces simultaneously. Furthermore, as the PCM's distance to the centre of the catalyst is reduced, the heat can penetrate more effectively to the catalyst's core. A similar catalyst volume (3 L) and PCM-graphite mixture mass (2 kg) have been taken into account for the optimized TES system design; however, this design can increase the cost of the aftertreatment system and also slightly increase the exhaust system's back pressure on the engine.

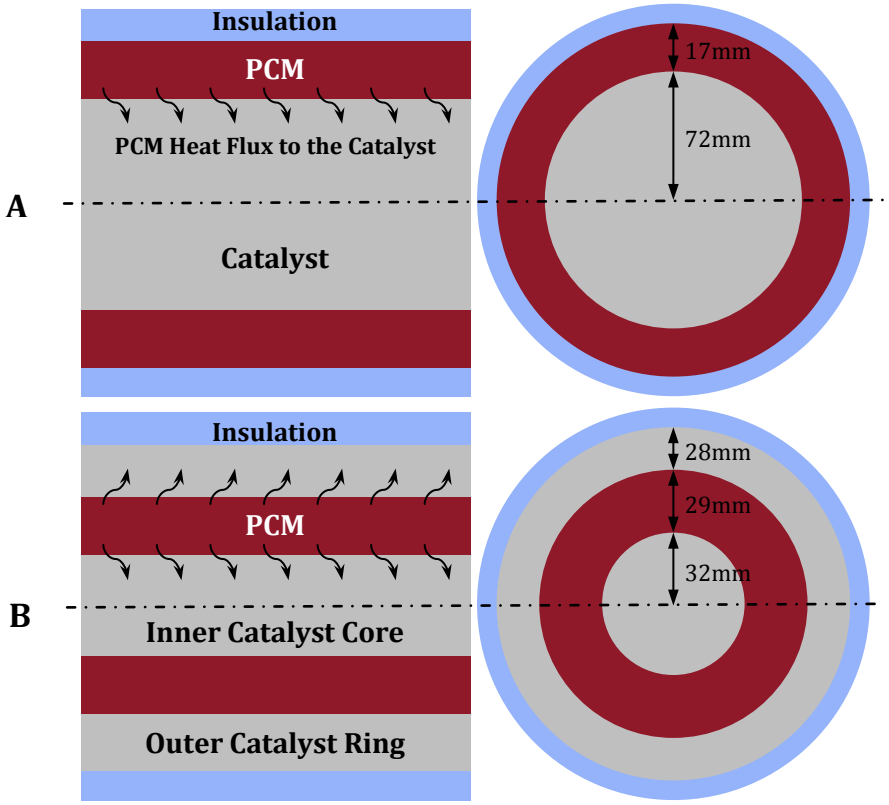

Figure 15: a) TES System Design with Outer PCM; b) Optimized TES System Design

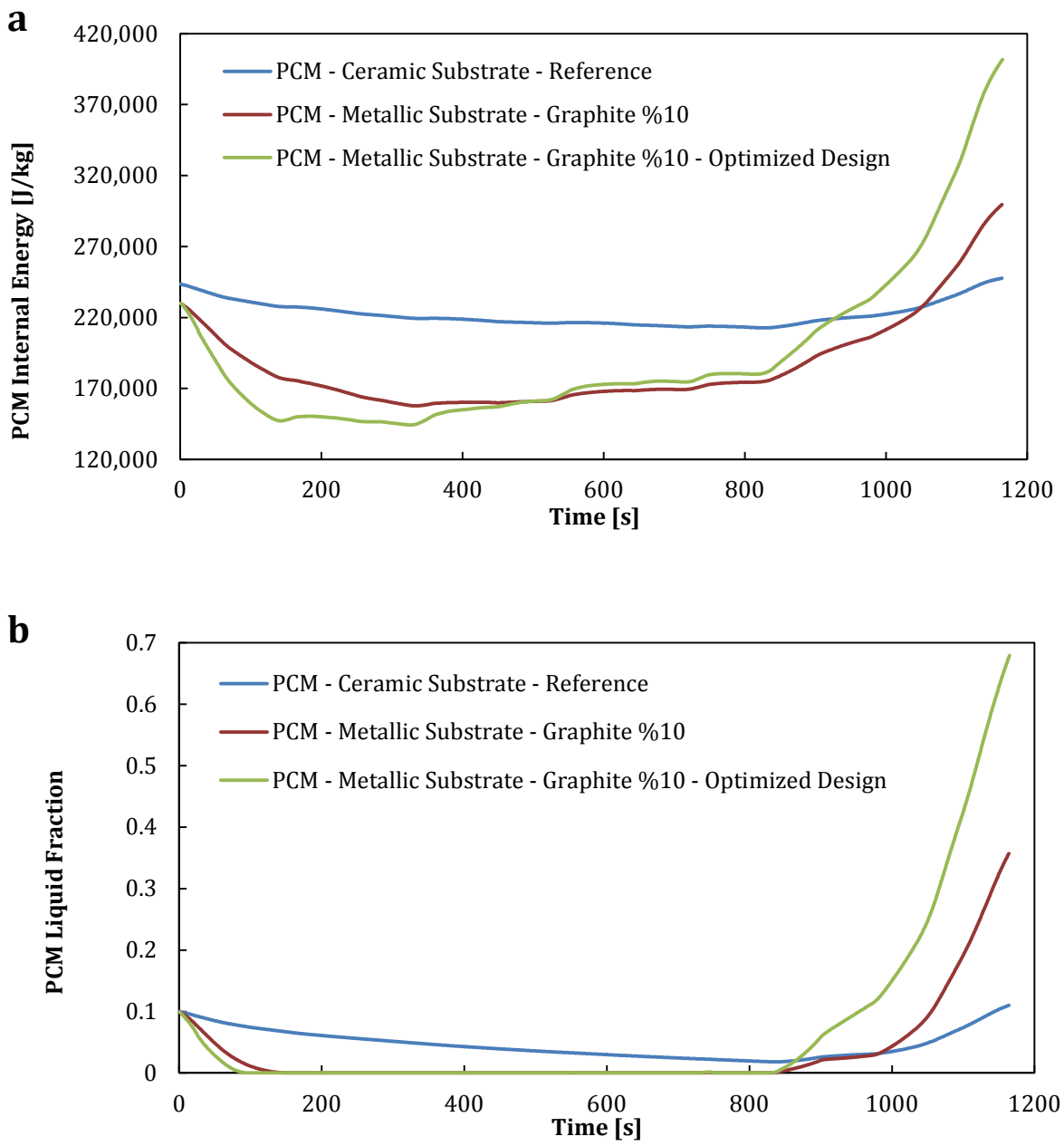

Figure 16: TES System Design Optimization Effect on the: (a) PCM's Internal Energy; (b) PCM's Liquid Fraction

Figure 16(a) shows that the optimized TES system design accelerates the PCM's thermal energy discharge during the cold-start compared to the improved TES system with the PCM-graphite mixture and metallic substrate. Moreover, this design optimization proved to further increase the total thermal energy delivered from the PCM to the aftertreatment system by 37% during the first 200 seconds of the NEDC.

Thermal energy storage performance of the optimized design has also improved significantly during the extra-urban part of the NEDC. As shown in Figure 16(b), the PCM's liquid fraction at the end of the NEDC can reach up to 0.68 for the optimized TES system, compared to 0.14 for the reference case and 0.36 for the case with improved materials. This can lead to an extended cooling period and enhanced emissions' conversion in the following driving cycle.

4. Conclusions

In this paper, a thermal energy storage (TES) system was introduced into the aftertreatment system to maintain the catalyst activated during engine-off periods for maximum cold-start emissions' conversion. This system includes a phase change material (PCM) mixture to store the excessive thermal energy and vacuum insulation to minimize the heat loss. The TES system was designed, investigated and optimized based on a light-duty diesel vehicle's aftertreatment requirements.

Preliminary investigations showed that the TES system is not able to provide sufficient thermal energy to the aftertreatment system in a timely manner, and the catalyst tends to light-out after around 85 seconds from the start of the NEDC. Therefore, different PCM additives and catalyst substrate materials were examined to increase the heat transfer rate between the PCM and the catalyst.

Adding 10% graphite by mass to the PCM mixture showed a significant increase in the PCM's thermal conductivity, which leads to an improved PCM thermal energy discharge during the cold-start. In conjunction with the PCM-graphite mixture, the ceramic catalyst substrate was substituted with a comparable metallic substrate that

features considerably higher thermal conductivity. This resulted in further improvement in the TES system's thermal behaviour, particularly in storing the excessive thermal energy during the extra-urban part of the NEDC. The improved TES system proved to reduce the cumulative CO and THC emissions by 91.7% and 41.2% respectively.

The TES system's cooling behaviour was also investigated to evaluate its thermal energy retention capability. Based on the results, 2 kg of the fully melted PCM mixture can maintain its liquid fraction above 0.1 for approximately 8 hours and 49 minutes when the engine is off in an atmospheric temperature of 25 °C. It can also maintain the catalyst's temperature above 150 °C for 12 hours and 53 minutes. It was concluded that the TES system's effective cooling period can be extended by approximately 4 hours and 25 minutes by increasing the PCM mixture's mass by 1 kg.

Lastly the TES system's design was optimized by utilizing an annular PCM reservoir that was accommodated in between two catalysts for improved heat transfer. The results indicated that this optimization can improve the TES's thermal behaviour and approximately double the PCM's liquid fraction at the end of the NEDC.

Acknowledgment

Jaguar Land Rover and the University of Birmingham are gratefully acknowledged for a financial grant to Mohammadreza Hamedi. Jaguar Land Rover is also acknowledged for technical support.

Nomenclature

Abbreviations

CFD	Computation fluid dynamics	H	Hydrogen
Cpsi	Cells per square inch	H	Enthalpy $(J.kg^{-1})$
DOC	Diesel oxidation catalyst	h	Sensible enthalpy $(J.kg^{-1})$
DPF	Diesel particulate filter	ΔH	Latent heat $(J.kg^{-1})$
IC	Internal combustion	HC	Hydrocarbon
NEDC	New European driving cycle	L	Latent heat $(J.kg^{-1})$
NMHCs	non-methane hydrocarbons	Mil	Milli-inch
PCM	Phase change material	N_2	Nitrogen
PM	Particulate matter	NO_x	Nitrogen oxides
SCR	Selective catalytic reduction	O_2	Oxygen
TES	Thermal energy storage	S	Source term
THS	Thermal hybrid system	T	Temperature (K)
TWC	Three-way catalyst	t	Time (s)
UDF	User define function	xGnP	exfoliated graphite Nano-platelets
Symbols		*Greek Symbols*	
C	Carbon	β	Liquid fraction
C_p	Specific heat capacity $(J.kg^{-1}K^{-1})$	λ	Thermal conductivity $(W.m^{-1}.K^{-1})$
CH_4	Methane	ρ	Density $(kg.m^{-3})$
CO	Carbon monoxide	$\vec{v}$	Fluid velocity
CO_2	Carbon dioxide		
H_2O	Water		

References

1. Chang Hwan Kim, Michael Paratore, Eugene Gonze, Charles Solbrig, and Stuart Smith, *Electrically Heated Catalysts for Cold-Start Emissions in Diesel Aftertreatment*. 2012, SAE International.

2. P. Rounce, A. Tsolakis, and A. P. E. York, *Speciation of particulate matter and hydrocarbon emissions from biodiesel combustion and its reduction by aftertreatment.* Fuel, 2012. **96**: p. 90-99.

3. Mohammad Reza Hamedi, Athanasios Tsolakis, and Jose Martin Herreros, *Thermal Performance of Diesel Aftertreatment: Material and Insulation CFD Analysis*. 2014, SAE International.

4. Stefano Cordiner, Vincenzo Mulone, Matteo Nobile, and Vittorio Rocco, *Impact of biodiesel fuel on engine emissions and Aftertreatment System operation.* Applied Energy, 2016. **164**: p. 972-983.

5. M. Gumus, *Reducing cold-start emission from internal combustion engines by means of thermal energy storage system.* Applied Thermal Engineering, 2009. **29**(4): p. 652-660.

6. E Korin, R Reshef, D Tshernichovesky, and E Sher, *Reducing cold-start emission from internal combustion engines by means of a catalytic converter embedded in a phase-change material.* Proceedings of the Institution of Mechanical Engineers, Part D: Journal of Automobile Engineering, 1999. **213**(6): p. 575-583.

7. Karthik Ramanathan, David H. West, and Vemuri Balakotaiah, *Optimal design of catalytic converters for minimizing cold-start emissions.* Catalysis Today, 2004. **98**(3): p. 357-373.

8. R.M. Heck, R.J. Farrauto, and S.T. Gulati, *Catalytic air pollution control: Commercial technology*. 2009: John Wiley & Sons, Inc.

9. Christos Dardiotis, Giorgio Martini, Alessandro Marotta, and Urbano Manfredi, *Low-temperature cold-start gaseous emissions of late technology passenger cars.* Applied Energy, 2013. **111**: p. 468-478.

10. Yuanwang Deng, Huawei Liu, Xiaohuan Zhao, Jiaqiang E, and Jianmei Chen, *Effects of cold start control strategy on cold start performance of the diesel engine based on a comprehensive preheat diesel engine model.* Applied Energy, 2018. **210**: p. 279-287.

11. Xiaohu Yang, Qingsong Bai, Zengxu Guo, Zhaoyang Niu, Chun Yang, Liwen Jin, Tian Jian Lu, and Jinyue Yan, *Comparison of direct numerical simulation with*

volume-averaged method on composite phase change materials for thermal energy storage. Applied Energy, 2018. **229**: p. 700-714.

12. Joris Jaguemont, Noshin Omar, Peter Van Den Bossche, and Joeri Mierlo, *Phase-change materials (PCM) for automotive applications: A review.* Applied Thermal Engineering, 2018. **132**: p. 308-320.

13. Huili Zhang, Jan Baeyens, Gustavo Cáceres, Jan Degrève, and Yongqin Lv, *Thermal energy storage: Recent developments and practical aspects.* Progress in Energy and Combustion Science, 2016. **53**: p. 1-40.

14. D. Zhou, C. Y. Zhao, and Y. Tian, *Review on thermal energy storage with phase change materials (PCMs) in building applications.* Applied Energy, 2012. **92**(Supplement C): p. 593-605.

15. Steven D. Burch, Thomas F. Potter, Matthew A. Keyser, Michael J. Brady, and Kenton F. Michaels, *Reducing Cold-Start Emissions by Catalytic Converter Thermal Management*. 1995, SAE International.

16. Eman-Bellah S. Mettawee and Ghazy M. R. Assassa, *Thermal conductivity enhancement in a latent heat storage system.* Solar Energy, 2007. **81**(7): p. 839-845.

17. Jinglei Xiang and Lawrence T. Drzal, *Investigation of exfoliated graphite nanoplatelets (xGnP) in improving thermal conductivity of paraffin wax-based phase change material.* Solar Energy Materials and Solar Cells, 2011. **95**(7): p. 1811-1818.

18. Sangki Park, Seungchul Woo, Jungwook Shon, and Kihyung Lee, *Experimental study on heat storage system using phase-change material in a diesel engine.* Energy, 2017. **119**: p. 1108-1118.

19. Sangki Park, Seungchul Woo, Jungwook Shon, and Kihyung Lee, *Numerical model and simulation of a vehicular heat storage system with phase-change material.* Applied Thermal Engineering, 2017. **113**: p. 1496-1504.

20. D. Vittorini, D. Di Battista, and R. Cipollone, *Engine oil warm-up through heat recovery on exhaust gases – Emissions reduction assessment during homologation cycles.* Thermal Science and Engineering Progress, 2018. **5**: p. 412-421.

21. Steven D. Burch, Matthew A. Keyser, Chris P. Colucci, Thomas F. Potter, David K. Benson, and John P. Biel, *Applications and Benefits of Catalytic Converter Thermal Management*. 1996, SAE International.

22. E. Korin, R. Reshef, D Tshernichovesky, and E Sher, *Reducing cold-start emission from internal combustion engines by means of a catalytic converter embedded in a*

phase-change material. Proceedings of the Institution of Mechanical Engineers, Part D: Journal of Automobile Engineering, 1999. **213: 575-583**.

23. Gerd Gaiser and Christian Seethaler, *Zero-Delay Light-Off - A New Cold-Start Concept with a Latent Heat Storage Integrated into a Catalyst Substrate*. 2007, SAE International.

24. Malik Monu, Dincer Ibrahim, and Rosen Marc A., *Review on use of phase change materials in battery thermal management for electric and hybrid electric vehicles.* International Journal of Energy Research, 2016. **40**(8): p. 1011-1031.

25. Rui Zhao, Sijie Zhang, Jie Liu, and Junjie Gu, *A review of thermal performance improving methods of lithium ion battery: Electrode modification and thermal management system.* Journal of Power Sources, 2015. **299**: p. 557-577.

26. Ziye Ling, Zhengguo Zhang, Guoquan Shi, Xiaoming Fang, Lei Wang, Xuenong Gao, Yutang Fang, Tao Xu, Shuangfeng Wang, and Xiaohong Liu, *Review on thermal management systems using phase change materials for electronic components, Li-ion batteries and photovoltaic modules.* Renewable and Sustainable Energy Reviews, 2014. **31**: p. 427-438.

27. Yvan Dutil, Daniel R. Rousse, Nizar Ben Salah, Stéphane Lassue, and Laurent Zalewski, *A review on phase-change materials: Mathematical modeling and simulations.* Renewable and Sustainable Energy Reviews, 2011. **15**(1): p. 112-130.

28. Ahmad Mustaffar, Adam Harvey, and David Reay, *Melting of phase change material assisted by expanded metal mesh.* Applied Thermal Engineering, 2015. **90**: p. 1052-1060.

29. Vinod M Janardhanan and Olaf Deutschmann, *Computational Fluid Dynamics of Catalytic Reactors*, in *Modeling and Simulation of Heterogeneous Catalytic Reactions*, O. Deutschmann, Editor. 2011.

30. Francois Lafossas, Yoshifumi Matsuda, Ali Mohammadi, Akinori Morishima, Mikio Inoue, Maria Kalogirou, Grigorios Koltsakis, and Zissis Samaras, *Calibration and Validation of a Diesel Oxidation Catalyst Model: from Synthetic Gas Testing to Driving Cycle Applications.* SAE International Journal of Engines, 2011. **4**(1): p. 1586-1606.

31. Turgut M. Gür, *Comprehensive review of methane conversion in solid oxide fuel cells: Prospects for efficient electricity generation from natural gas.* Progress in Energy and Combustion Science, 2016. **54**: p. 1-64.